NASA-CR-198856

High Resolution X-ray Spectroscopy From Sounding Rockets NSG 5-96

Final Report July 7, 1995

Principal Investigator Webster Cash, Professor of Astrophysics
Center for Astrophysics and Space Astronomy
Campus Box 389
University of Colorado
Boulder CO 80309 (303) 492-4056

I. PROGRAM HISTORY

This program is the merging of two established programs in sounding rocket X-ray Astronomy. The Lockheed effort has centered on a meter class x-ray optic for the Aries rocket. The Colorado effort has focused on a smaller Black Brant payload, but there has been considerable interaction between the two programs for the last ten years. Both programs have been quite active since the last peer review three years ago. This section summarizes the activity in that period.

Aries Payload

The Aries payload XOGS (X-ray Objective Grating Spectrograph) featured three nested Wolter I telescopes cut from aluminum and lacquer coated for polish. An array of twelve huge gratings (12x50cm) diffracted light in the off-plane mount down into the telescope aperture. The spectra so formed were recorded by a Penning Gas Imager (from Mullard Space Sciences Laboratory) in the focal plane. The system achieved $10cm^2$ of effective area and spectral resolution of about 75 ($\lambda/\delta\lambda$).

XOGS was first launched in May, 1991 from the White Sands Missile Range to observe Scorpius X-1. The Aries functioned perfectly, but there were two problems with the detector. A coronal discharge killed the detector preamps, but the Wallops Island detector door squibs had failed to operate anyway. Thus no signal was received. The failures were analyzed and fixed. In June 1993 we took XOGS to the High Energy Laser Test Facility (HELSTF) 300meter beam facility at White Sands. We had a very interesting calibration run, in which we learned a great deal about calibrating high resolution spectrographs in the x-ray. Figure 1 is a sample spectrum, showing both emission and absorption features.

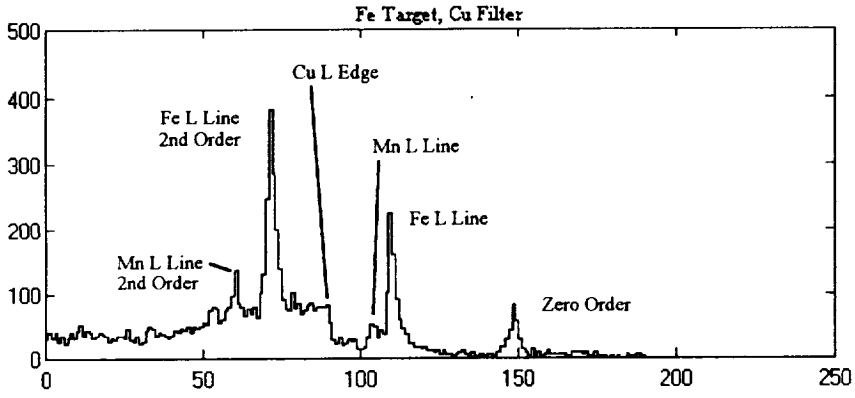

Figure 1: XOGS calibration spectrum obtained at the HELSTF facility in New Mexico. In this run we used an Fe target, which turned out to have manganese in the alloy. The beam passed through a thin copper filter to remove low energy bremsstrahlung and create the absorption edge.

After calibration, XOGS was integrated into an Aries and launched on August 28th with the oxygen edge in the Crab nebula as its target. Unfortunately, at 28 seconds after launch, a nozzle on the Aries broke apart, and the flight reached a peak altitude of only five miles. This, being so low, prevented the parachute from deploying, and XOGS free fell, landing less than a mile from the tower. The payload was scattered over several acres of desert. R.I.P. X.O.G.S.

Astro-Spas Study

In 1991 XOGS was chosen as the payload for the third flight of the Astro-Spas, the German-American shuttle based free-flyer, on which ORFEUS and IMAPS are the first payloads. We performed a full study, identifying how to raise the throughput to 100cm^2, and fly within three years. The potential scientific return was exciting.

Unfortunately, the costs of converting anything to meet specification for the shuttle is steep, in this case, even factoring in contributions from the British, the cost was $5 million, and NASA was unable to find the funds. Instead, the third Astro-Spas flight will be a reflight of Astro-Spas number one, the ultraviolet mission.

Black Brant Payload

The Black Brant payload has had better luck. For this payload we built a 30cm aperture un-nested Wolter I telescope in-house, using grind and polish techniques. It has 58cm^2 of geometric collecting area, and about 30 arcseconds resolution at 1keV. At the focal plane is a one inch diameter micro-channel plate with resistive anode readout.

The first flight of this payload was March 18, 1991. In that flight we created an aperture stop which masked the entrance annulus of the optic. This aperture, because of the anisotropic nature of grazing optics, created a Maltese Cross shaped image in the focal plane. By using the effects of off-plane imaging in this way, we could much better separate the scattering of the telescope from the scattering of interstellar dust grains. We targeted Sco X-1 for our dust grain study because of a) its brightness, and b) ROSAT would not observe it. The flight was a success, although the telescope went a little out of focus due to thermal stresses, and the background was high due to a filter leak at 304Å. The Maltese Cross image of Sco is shown in Figure 2.

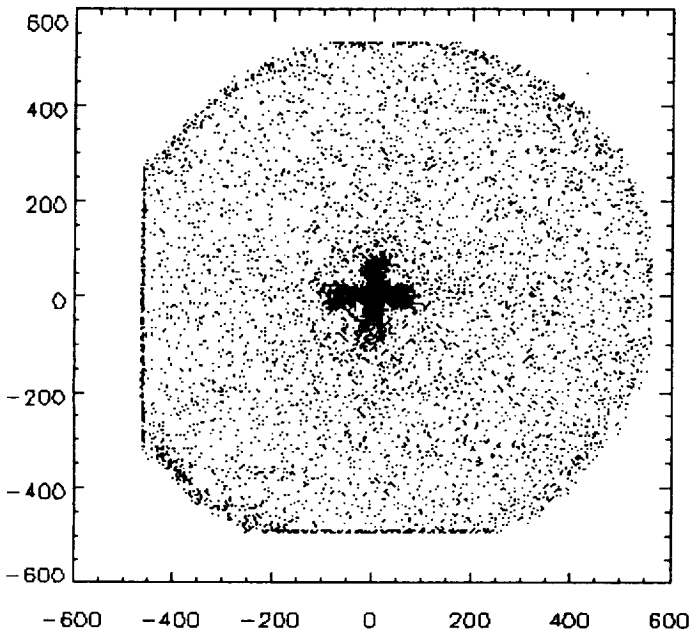

Figure 2: flight image of Scorpius X-1 obtained in a rocket flight on March 18, 1991. The Maltese Cross is the result of apodization of the entrance annulus.

We were unable to detect the halo of Sco X-1, but we were able to show that the reddening was lower than measured by some techniques, most notably by scaling from the depth of the 2200Å absorption feature. This paper has been recently submitted to the Astrophyiscal Journal. A reflight with a better filter would be able to push the limit much lower.

The second flight was on January 31, 1992. ROSAT had just released the first x-ray image of the Moon. They interpreted the flux as low level direct reflection from the surface. The prediction then was that the crescent Moon would be much brighter, as the x-rays would be scattering off the surface at grazing incidence. This flight worked perfectly, but, unfortunately, the Moon does *not* get brighter at the crescent phase. Our result is now being combined with EUV and X-ray data to constrain the overall scattering function of the lunar surface.

The third flight was April 15, 1993. For this flight we added four diffraction gratings to the front of the payload to create a small version of XOGS. We calibrated in the HELSTF beam in March, prior to launch. Indeed, it was on this run that we developed and tested most of the beam techniques that we subsequently applied to XOGS. The flight was fully successful, recording a spectrum of ScoX-1 with

resolution of 100. Analysis is underway, and currently indicates that the spectrum was devoid of strong feature at the time we flew. While there is a hint of some weak features, requiring detailed statistical analysis, we can at this time state that there were no sharp lines that carried over 1% of the total 0.5-2.0keV flux from Sco.

The major lesson we learned from our activities, the lesson that lies at the foundation of our new telescope designs, is that we need high collecting area in a compact package if we are to produce high quality spectra. We believe that the new optics described in this proposal will meet that need.

II. SPHERES AT GRAZING INCIDENCE

As part of this effort we developed a new, promising approach to x-ray optics.

Spheres At Grazing Incidence

The big problem with grazing incidence optical systems is in the building of telescopes. In previous years, missions may have had difficulties with detectors, but advances in CCD technology now assure X-ray missions inexpensive, high quality detectors. A series of missions including the Apollo Telescope Mount, Einstein, ROSAT, and now AXAF, have all achieved X-ray spatial imaging in the 1 to 10 arcsecond quality range, but only at the price of years of effort and tens of millions of dollars. While this approach widely demonstrated the utility of grazing incidence optics, and established the importance of X-ray astronomy, the price was, and still is, prohibitive for all but the very best funded programs in the world. Furthermore, the debilitating cost of approaching one arcsecond performance with Wolter telescopes has effectively blocked any attempt to move beyond, into the subarcsecond range. Clearly, an approach to sub arcsecond optics that is practical and affordable is desperately needed.

In the early days of automobiles, each car was laboriously assembled on an individual basis, and the cost was such that they were considered oddities -- playthings for the very rich. Henry Ford, through his inventive techniques of mass production, made the automobile available at low cost, and the industry changed. What we need for X-ray astronomy is a Model T X-ray telescope.

Gorenstein (1992) has recently written a brief review of the alternatives to the "traditional" Wolter optics. His purpose in reviewing non-traditional optics was similar to ours, in that there is a clear need to identify optical techniques with the potential to carry us beyond the current generation of observatories into new regions of collecting area, resolution, and field of view. He found no one approach that was outstanding. Instead, he did identify some techniques with potential for specific applications only.

So what is the stumbling block that makes the telescopes so expensive? Here at CU we have been building Wolter optics and flying them on sounding rockets. We have used the approach of subcontracting to industry. We have also fabricated them ourselves. In both approaches we have found the telescope to be the most time consuming and expensive portion of the payload. From our direct experience we know the reason to be in the figure and polish stage of the fabrication. The extreme difference in the two radii of curvature in the paraboloid and hyperboloid makes a small lapping tool necessary. This in turn makes it very difficult to control figure, particularly in the millimeter scale range. Extreme care and long hours are necessary to carefully bring the figure in, and then to polish without hurting the figure.

Of course, this experience is the same well-known problem of the AXAF project. Through massive, continuing efforts, it has been possible to create a one arcsecond level telescope. Yet, the tolerances achieved in polish and figure are still short of a conventional normal incidence sphere.

It occurred to us that the answer to this problem lies not in improving the technology of polish and figure on extreme asphere optics, but in learning to work with shapes that we already know how to figure and polish to high precision. We took a more careful look at using normal incidence spherical telescopes at grazing incidence. We discovered a new class of telescope that is extremely practical to build and has the potential of greatly exceeding the resolution of AXAF.

Behavior of Single Spheres

We start with a conventional spherical mirror and assume it is roughly square in its dimensions. When tilted over to a typical graze angle of two degrees, it presents a long, narrow entrance aperture. For the

sake of clarity, let us assume that is roughly 30cm across. This makes the entrance aperture 30cm long and 1cm wide.

If the mirror is concave, it will provide a low quality focus at a distance of $R\sin\theta/2$. If we desire a typical focal length of 200cm, R must be about 100 meters. The focus will be very nearly a straight line, since the curvature in the other direction is only a few microns over the entire 30cm length. In other words, the sphere is almost indistinguishable from a cylinder in focus terms. Similarly, because this is an f/300 sphere, the spherical surface is indistinguishable from a paraboloid. Thus pure spheres are used throughout the design.

There are a few applications in which one dimensional imaging is adequate, but, for the most part, telescope applications require two dimensional imaging. This is accomplished by placing a second sphere perpendicular in the converging beam. Since the behavior is so close to that of a cylinder, there is almost no crossover between the two dimensions, and a two dimensional focus can be found.

A major problem that subsequently arises for celestial X-ray astronomy is that the entrance aperture has been reduced to about one square centimeter. The solution to this is to align a series of spheres in parallel, the one-dimensional analog of nesting paraboloids. When this is done in both layers, high collecting areas can be achieved.

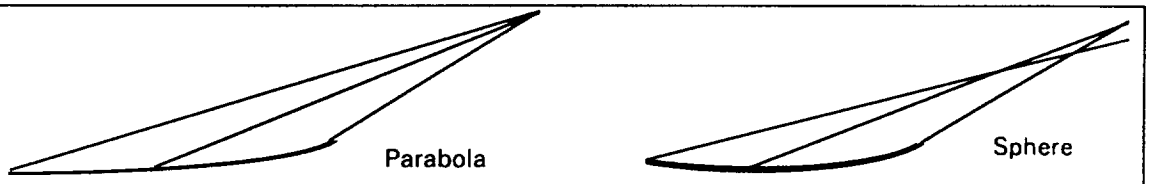

Figure 3: Above is a schematic of a grazing incidence parabola of the kind used in Wolter telescopes. Parallel light is focused to a perfect point. Below is the equivalent diagram for a conventional on-axis sphere used at grazing incidence. There is a severe spherical aberration that limits resolution.

Spherical Correctors

The principal drawback to single spheres is the poor quality of the focus. The deviation of the spheres from the grazing paraboloid is significant, as shown schematically in Figure 3. While parabolas and spheres are nearly identical in slow systems as mentioned above, this is true only near their respective vertices. The *grazing incidence* portion of a parabola has an asymmetry not matched by a sphere, creating the primary aberration found in spheres at grazing incidence.

It occurred to us that perhaps another sphere, properly positioned and oriented relative to the first sphere, might be able to take the poor focus, and refocus it, simultaneously removing the worst of the

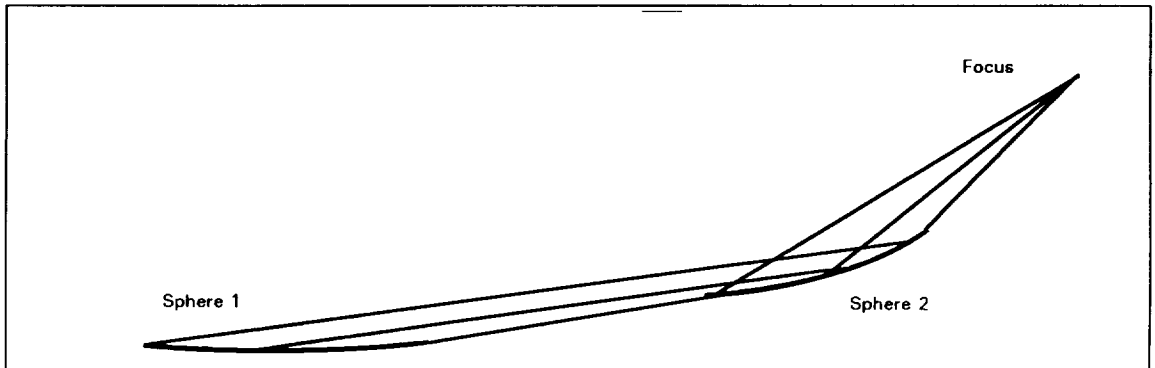

Figure 4: This shows schematically a two sphere layout that produces a high quality line focus. Since both surfaces are concave, the reflection angles are additive, and the beam from the first is intercepted by the second before the focus. This arrangement is an analog of the Wolter Type I.

aberrations. We have been able to establish that this is, in fact, not only possible, but relatively simple to implement. Furthermore, entire classes of geometries exist, analogs of the Wolter Types I, II and III. The

solutions were initially found using raytrace optimization, searching blindly for a solution. Later, we were able to show algebraically that the solutions are correct. This result is in preparation for submission to Applied Optics (Cash, 1993).

The quality of the line focus thus formed came as a surprise. Many practical geometries turned out to have 0.1 or even 0.01 arcsecond imaging on axis. Indeed, the quality of focus was below the diffraction limit for many applications, since a 20Å beam across a 1cm aperture is diffraction limited at about .05". When the effects of scattering on a high quality sphere at grazing incidence are calculated, one again finds that standard numbers predict a scattering limit in the neighborhood of .01". In other words, for the first time, we have a practical means to fabricate diffraction limited X-ray optics!

It should be noted that to achieve a high quality, two-dimensional image, two mirrors are required in each dimension. The X-rays are required to pass through a four reflection system. Even with good polish, there will still be reflection losses in the surfaces, so the throughput per unit area of aperture will be somewhat lower than that of a Wolter telescope. However, since the price per unit area has dropped by two orders of magnitude, a factor of two loss in efficiency is acceptable.

III. EXAMPLE USE OF SPHERES

Overview

We are proposing to build the first of the next generation of dispersive spectrographs for soft x-ray astronomy. The payload has been conceived with the goal of achieving very high collecting area 30-80cm^2 *effective* coupled with resolution of at least 200 ($\lambda/\delta\lambda$), and doing it within the physical and financial constraints of a sounding rocket. With this capability we will have the ability to seriously study the spectra of many of the brighter x-ray sources starting in about 18 months.

The instrument will feature an all-spherical telescope as described in Section IV, but will have only one layer of mirrors in each dimension. The lack of correctors limits the spatial resolution to about 2 arcseconds, but this is excellent for spectroscopy. The gratings will be replicas of an existing radial groove grating master, that has already been flown in an Extreme Ultraviolet Spectrograph rocket (Cash, 1983, Wilkinson et al, 1993). The detector is a CCD with 24micron pixels and 100eV energy resolution that is ideal for separating order confusion.

The optics have been made long to maximize performance. We are assuming a 4meter payload, which Wallops Flight Facility indicates is acceptable. By using a CCD, there is no need for high voltage, removing high vacuum requirements from the payload. All the components are now reasonably standard except for the telescope. We estimate that the spheres can be fabricated, and co-aligned within about one year. Launch should follow in six months.

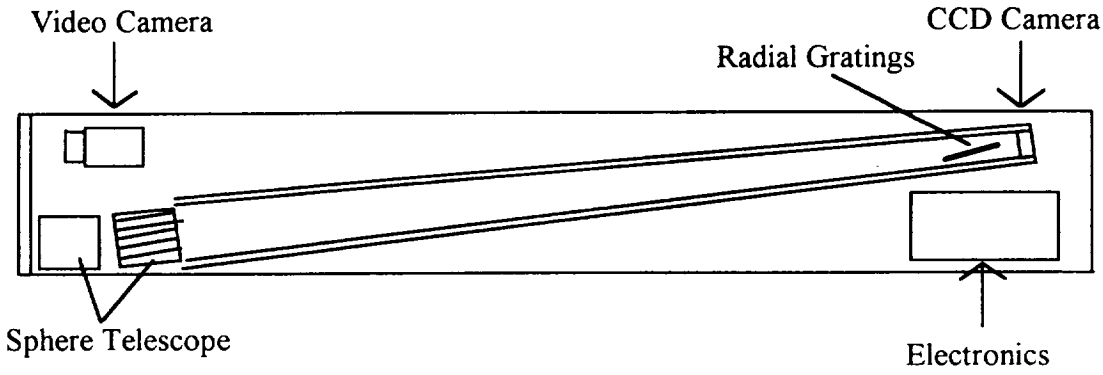

Figure 5: Schematic of proposed payload layout showing the locations of the various components inside a standard 22" NASA sounding rocket skin. This schematic is for the one or two module version we intend to fly first.

Telescope Design And Fabrication

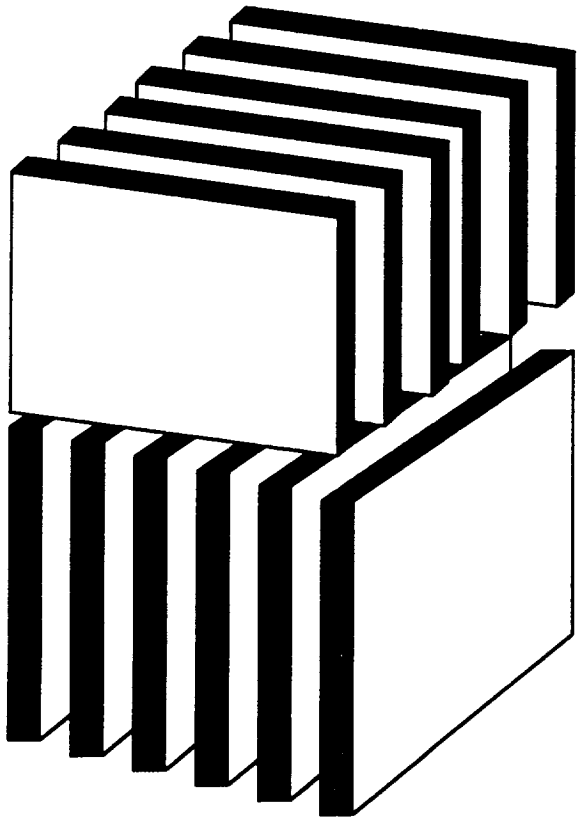

Figure 6: The spherical mirrors are laid out in a linear geometry, with two layers, one for each dimension.

The telescope design that we have developed for our spectroscopy is based on 22 six inch square spherical surface telescopes. There are eleven mirrors in each of the two layers. The thickness of each mirror is crucial to the efficiency of the system. We are expecting that to maintain the figure and mechanical strength a thickness of 10mm is adequate. However, at a graze angle of 2 degrees, the thickness of the open aperture for a 15cm plate is only 5mm. Thus, in each dimension, only one third is optical surface, yielding just over 10% total efficiency. The array has 121 square apertures of 0.25cm^2 each, for a total of 30cm^2 geometric area. This is excellent, considering that the 30cm diameter Wolter we have been flying on the Black Brant has only 58cm^2 geometric.

Layer 1 Mirror Parameters

Mirror	Off Center (mm)	Graze Angle (deg)	Radius (mm)
1	75.	2.5336	180000.
2	60.	2.4271	189461.
3	45.	2.3204	197707.
4	30.	2.2136	207442.
5	15.	2.1067	218632.
6	0.	2.0000	229832.
7	-15.	1.8931	242444.
8	-30.	1.7860	256533.
9	-45.	1.6791	271949.
10	-60.	1.5719	292329.
11	-75.	1.4646	319161.

Layer 2 Mirror Parameters

Mirror	Off Center (mm)	Graze Angle (deg)	Radius (mm)
1	75.	2.6558	162894.
2	60.	2.5435	172512.
3	45.	2.4310	180089.
4	30.	2.3183	189768.
5	15.	2.2057	198501.
6	0.	2.0930	208832.
7	-15.	1.9802	220224.
8	-30.	1.8673	233050.
9	-45.	1.7544	248975.
10	-60.	1.6414	265670.
11	-75.	1.5284	285036.

Layer 3 - Gratings

Grating	Angle (deg)	Offset (mm)	line/mm/Å	blaze (deg)
1	1.10	15.	7.55	20.
2	2.20	15.	7.55	20.

Raytracing

The telescope has been fully raytraced. Indeed, the parameters of the many spheres were found using the optimization routine of the raytracer. The telescope has a 4 meter focal length and a FWHM focus of 50 microns, nicely matched to the 24 micron resolution of the CCD. Thus, the spectral resolution is about 20 times the dispersion distance (in mm). Since most of our light will be about 12 mm from zero order, we expect resolution of 240. It should be noted, however, that if we were to place the gratings immediately below the telescope, we would need a lot more gratings, but we would achieve dispersion high enough to support resolution ($\lambda/\delta\lambda$) of 5000!

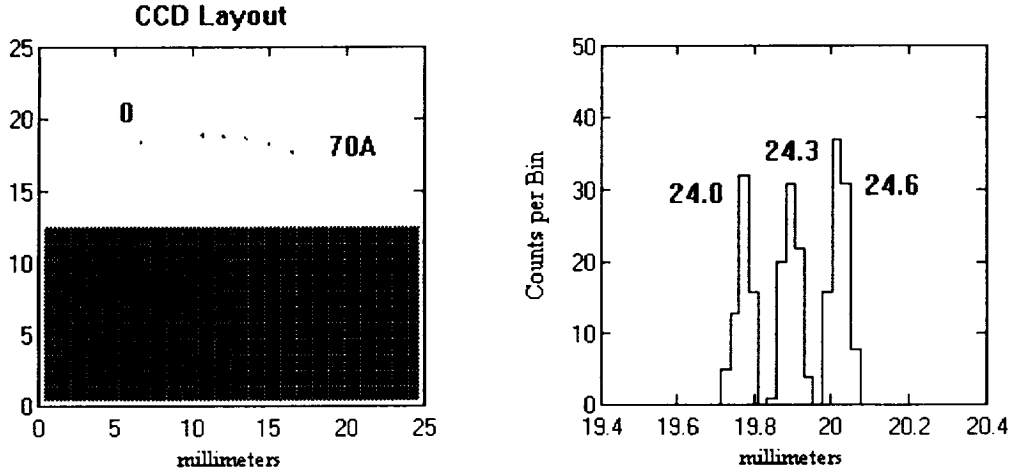

Figure 7: To the left is a raytrace that shows the spectrum as it might appear on the one inch CCD. The lower half of the CCD is shielded, to become the area into which the signal is quickly shifted for readout. At right is a histogram formed from the raytrace, it shows three wavelengths of x-rays (24, 24.3 and 24.6Å) with resolution of about 200.

Tolerance Analysis

The ability to meet the surface finish tolerance requirements for 2.0 arcsecond image with the spheres is straight forward and poses little risk with current spherical optics polishing techniques. The telescope design utilizes all the advantages of low surface scatter from the grazing incidence mount. Each sub image from the telescope is formed by reflection off of two long radius spheres at grazing incidence. The equation that describes the scattering from two reflections is

$$S_{total} = 2S - S^2$$

where S is the scattering from a single surface and each surface scatters equally. Figure 8 shows a plot of the Total Integrated Scattering (TIS) curve for two 2° graze angle reflections as a function of the single surface RMS micro surface roughness at a wavelength of 20Å. First order Beckmann theory was used (Beckmann, 1963).

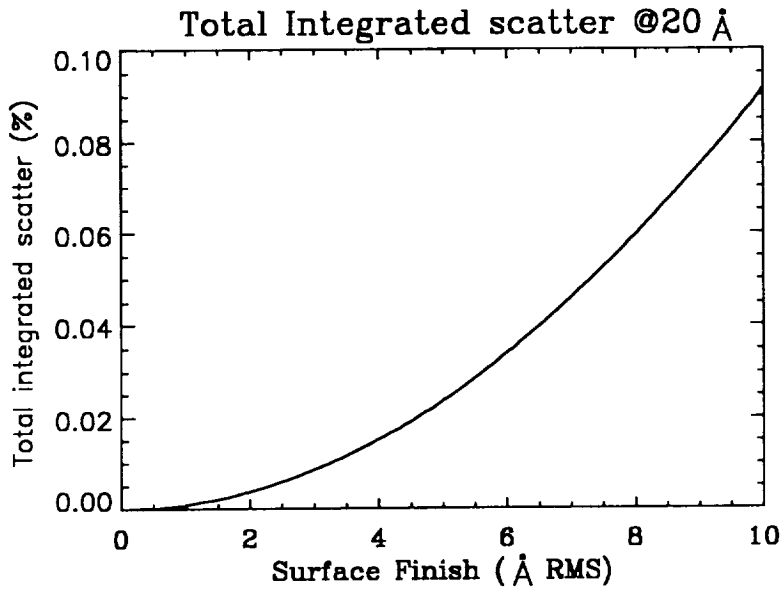

Figure 8: Total Integrated Scatter (TIS) for the all spherical X-ray telescope/spectrograph as a function of the surface finish of a single mirror. Two grazing incidence reflections of 2° at a wavelength of 20Å were used for the plot.

It can be shown from figure 11 that our spherical X-ray telescope will have very low scatter. As discussed earlier from raytracing results the two reflection spherical system will have 2 arcsecond aberration limited imaging capability. The following equation describes the relation between surface scatter and figure error correlation length in the small angle approximation.

$$\rho = \frac{\lambda}{\theta_{scatter}\theta_{graze}}$$

where ρ is the correlation length of the figure error, λ the wavelength, $\theta_{scatter}$ the scattering angle and θ_{graze} the reflection graze angle. From the above equation, at 20Å with $\theta_{graze}=2^\circ$ the maximum correlation length for scattering inside 2 arcseconds is ρ=6 mm. Current polishing technology for spherical optics have micro surface roughness in the 2-3 Å RMS range for correlation lengths $\cong$1-5 mm (Spiller, 1990; Baker, 1990). Thus we can expect total scattering in angles greater than 2 arcseconds to be less than 1% or, in other words, a virtually scatter free x-ray telescope. Even with surface roughness as high as 10Å RMS we can still expect 90% inside 2 arcseconds, and a 10Å RMS is easily achievable in any standard optics shop. Figure errors with correlation lengths greater then 6 mm affect imaging inside 2

arcseconds and thus can be treated by geometric optics and only need to fit the design sphere to within about 1 arcsecond or about 2 fringes when tested by interferometry at 6328Å . Thus, we see no imaging problems as a result of figuring errors using current optical manufacturing techniques.

Fabrication of the Spheres

The spherical optics closely resemble flats because of their long radii and so the techniques used for fabrication would be similar. The measurement of radius and figure quality for a sphere can be performed under the same interferometric setup commonly used for testing optical flats against a high quality reference flat. For example, mirror 1 of the first mirror assembly has a radius of 180 meters. This corresponds to a sagittal depth of 31.25μ assuming an optic diameter of 150 mm. This amounts to 49.38 waves of departure from a flat which would show as a bulls eye pattern consisting of 49 and 1/3 concentric rings under interferometric testing (see Figure 12). Current optical metrology technology is capable of achieving sagittal depths for ~150 meters radius spheres to about $\lambda/4$ at 6328Å which translates to maintaining radius to within 1%. Maintaining radius accuracy to these tolerances would meet the tolerances of the spectrograph telescope.

Our first step in fabricating the telescope would be to create the master spheres, one of each needed radius of curvature. These surfaces would be fabricated by standard techniques, and their actual radii measured directly. These masters would then be used as reference surfaces. Just as a flat mirror is polished in by referencing the optic to a standard flat, we will use the long radius masters. This will allow excellent quality spheres to be built with well controlled radii, at very low cost, similar to that of a flat mirror.

It is our intention to order the spheres from a standard optics shop, preferably one nearby so that we can work closely with the opticians. Nothing we are doing should require expensive, specialized work. The mirrors will be individually polished on a continuous polisher, using the null test against the masters. An experienced optician can easily do a batch of fifteen such mirrors in a two week run, so there should be no schedule difficulty even for a 300 mirror system.

Assembly and Alignment

Because the beams from the individual mirrors must meet to form a 2 arcsecond image, the relative alignment of the mirrors must be carefully controlled. The values are well known, but if the mirror shifts laterally, the angle must compensate. Thus there are two approaches to assembly. If the mirrors are assembled in a grazing incidence beam, the relative focus can be adjusted directly. However, the diffraction of a visible light beam is serious, broadening the focus to 400 microns, which will make alignment to 10 microns tough. If we use 2500Å light, then the number drops to 200 microns, and 10 microns sounds more feasible.

Alternatively, careful metrology may give us a more direct and controllable approach to assembly of the arrays. Figure 12 shows a schematic of the setup that could be used for aligning the mirror arrays. The sequence for assembly begins by gluing the first mirror in place with no tilt as seen by the output TV, rotate the table the prescribed amount for the next mirror and glue this mirror in place with no tilt. In order to know the correct angle, one must know the placement of the mirror, so this will be monitored by a digital micrometer during the alignment process. This sequence would be followed for all 15 mirrors in the first mirror assembly. The process is repeated for the second mirror assembly. The inter-alignment between the two mirror arrays for final assembly of the spectrograph telescope is not as critical and so does not require interferometry.

Glue will be used to mount the mirrors because of it permanency and its ability to induce smaller holding forces on the optics, allowing for thinner spheres and thus a high effective area telescope. The mirrors will be glued in an Invar structure (not shown in figure 12 for clarity) to minimize changes in the telescope imaging properties with temperature.

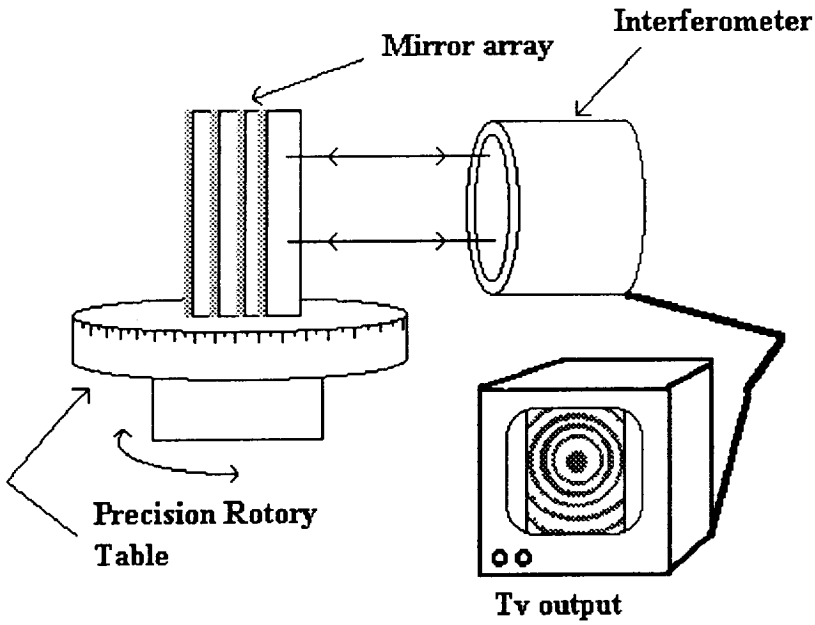

Figure 9 Schematic of interferometer setup for aligning and gluing each sphere. The rotary table is an off-the-shelf precision turn table capable of better than 1 arcsecond angle positioning. An off-the-shelf ZYGO interferometer is fully capable of performing all the necessary interferometry for telescope assembly.

Variations on the Telescope Design

The design presented above generates about 30cm^2 of geometric area from the 250cm^2 in the front square. The other 88% of the light entering this 6 inch cube strikes the edge of a mirror in either the front or the back layer. Thus, if the mirrors can be made thinner and stacked closer together, the throughput rises rapidly as shown in the table below.

Size (mm)	Thickness (mm)	No. Mirrors per layer	Geometric Area (cm^2)
160x160	10	11	30
160x160	6	15	55
160x160	3	20	100

It is clear that there is tremendous motivation to use blanks as thin as possible. The problem that arises from thin blanks is not in the figuring or polishing, but in maintaining the figure against deformation in the mounting process. We are certain that 10mm blanks are sufficiently stiff that they will not present any problems. We are reasonably confident that 150mm blanks, 6mm thick will be stable if treated gently. Thus our throughput estimates and science simulations are based on 55cm^2 geometric area per module. We *hope* to find a way to use one-eighth inch blanks (3mm), because of the 100cm^2 that they can generate.

To make the choice of thickness we will perform some simple laboratory studies on thin flats prior to ordering flight mirrors.